the concept that as much as possible, resection of glioma is the most effective treatment of the patients with glioma, especially with the high-grade glioma, like glioblastoma. The other crucial issue for longer survival is dependent on the treatment after recurrence. If the recurrence is located just adjacent to the primary site, additional resection of the recurrent part is the most effective mass reduction method compared to other modality, especially for gliomas which are intractable to chemoradiation therapy. After successful local control of the tumor, recurrent pattern changed into dissemination which condition is out of indication of surgical resection. In order to achieve the effective treatment after recurrence, we have to check the patients regularly and meticulously; that means regular control image diagnosis, especially by MRI. So, in this situation in Japan, all people living in Japan have the same chances to be checked evenly by the medical insurance with relative low cost. So the active and positive attitude for treatment of the patients with high-grade glioma is basically needed to achieve higher results of the overall survival of them. In this meaning, this paper stimulates neurosurgeons to be aware of the importance of active resection with contrivance for prevention of dissemination and meticulous follow-up of the patients with regular control study by MRI.

Jesús Vaquero, Madrid, Spain

In this review, Saito et al. describe their experience with a series of patients with intracranial anaplastic ependymomas who underwent more than subtotal resection and intensive treatment for recurrence, including surgery and chemoradiation. The authors conclude that this therapeutic approach improved survival, and suggest that tumor dissemination is the life-determining factor in their patients. This work is well-written and supports the appropriateness of an aggressive attitude when we are faced with an intracranial anaplastic ependymoma. However, the number of patients in the series is relatively small and is well-known that many different factors can influence the evolution and survival of patients suffering brain tumors. Therefore, the conclusions obtained in series as shown by the authors, although they are justified and are extremely useful in increasing our understanding, should be considered with caution.

One point to note is that this series includes both children and adults patients, being generally accepted that age is a very important factor when analyzing biological prognosis of intracranial ependymomas[1]. Furthermore, it is obvious that when a patient with an intracranial ependymoma is considered individually, age may condition the type and aggressiveness of adjuvant therapies after surgery.

Reference

1. Rodriguez D, Cheung MC, Housri N, Quinones-Hinojosa A, Camphausen K, Koniaris LG (2009) Outcomes of malignant CNS ependymomas: an examination of 2,408 cases through the Surveillance, Epidemiology, and End Results (SEER) database (1973-2005). J Surg Res 156: 340-351

Brain Tumor Pathol (2010) 27:51–57
DOI 10.1007/s10014-010-0263-y

CASE REPORT

Shunsuke Omodaka · Ryuta Saito · Toshihiro Kumabe
Jun Kawagishi · Hidefumi Jokura · Yukihiko Sonoda
Mika Watanabe · Takamasa Kayama · Teiji Tominaga

Melanotic neuroectodermal tumor of the brain recurring 12 years after complete remission: case report

Received: October 29, 2009 / Accepted: January 14, 2010

Abstract We describe a rare case of melanotic neuroectodermal tumor (MNT) of the brain recurring 12 years after complete remission. An 11-year-old girl initially presented with exotropia and bilateral papilledema. Magnetic resonance (MR) imaging revealed an intracranial extraaxial large tumor at the midfrontal region. T_1-weighted MR imaging showed the tumor to be well delineated with homogeneous enhancement by gadolinium. The tumor was subtotally removed, and the histological diagnosis was MNT. The residual tumor became enlarged, so gamma knife radiosurgery was performed 5 months after initial surgery. The enhanced lesion disappeared, but another lesion emerged 3 years later. A second gamma knife radiosurgery was performed for this local recurrence. The enhanced lesion disappeared once again. Twelve years after the second gamma knife radiosurgery, another local recurrence was detected. This tumor was subtotally removed. Histological examination confirmed the same diagnosis of MNT. This case suggests that MNTs not completely resected need long-term follow up, even if complete remission was achieved after adjuvant therapy.

Key words Melanotic neuroectodermal tumor of the brain · Recurrence · Gamma knife · Prognosis

S. Omodaka · R. Saito · T. Kumabe (✉) · Y. Sonoda · T. Tominaga
Department of Neurosurgery, Tohoku University Graduate School of Medicine, 1-1 Seiryo-machi, Aoba-ku, Sendai, Miyagi 980-8574, Japan
Tel. +81-22-717-7230; Fax +81-22-717-7233
e-mail: kuma@nsg.med.tohoku.ac.jp

J. Kawagishi · H. Jokura
Jiro Suzuki Memorial Gamma House, Furukawa Seiryo Hospital, Miyagi, Japan

M. Watanabe
Department of Pathology, Tohoku University Hospital, Miyagi, Japan

T. Kayama
Department of Neurosurgery, Faculty of Medicine, Yamagata University, Yamagata, Japan

Introduction

Melanotic neuroectodermal tumor (MNT) is a rare, pigmented tumor of neural crest origin, mainly affecting children under 1 year of age without sex predilection.[1,2] Peripheral MNTs are considered to be benign, whereas MNTs in the brain carry a much less favorable prognosis.[3] More than 365 cases have been reported since the first description in 1918.[3] A review of 140 cases of MNT reported between 1990 and 2004 found that the main site of origin was the maxilla (61.4%), followed by the skull (15.7%), the mandible (6.4%), and the brain (5.7%).[2] The treatment of MNT consists of total surgical excision and, if malignant, followed by radiation therapy and chemotherapy.[4] Most MNTs have a benign clinical course after surgical removal, but the local recurrence rate is reported to be as high as 20% and the rate of malignancy as 6.5%. Most recurrences after surgical treatment occur within 4 weeks (39.3%). No reported case has recurred more than 23 months after treatment. Local recurrences are explained as subtotal removal or multicentric origin of the tumor.[5] The recurrence rate of MNT after incomplete resection is as high as 60%.[6]

We describe a rare case of MNT of the brain that recurred 12 years after complete remission.

Clinical summary

An otherwise healthy 11-year-old girl had initially presented with diplopia caused by left exotropia and bilateral papilledema without other neurological deficits in July 1993. Computed tomography revealed a large, approximately 6 cm in maximum diameter, rounded tumor in the intracranial midfrontal region. Magnetic resonance (MR) imaging revealed a well-delineated extraaxial tumor compressing the bilateral frontal lobes with marked intracerebral edema (Fig. 1a–c). The tumor was isointense with the cortex on both T_1- and T_2-weighted MR images, with strong homogeneous enhancement with dural enhancement after

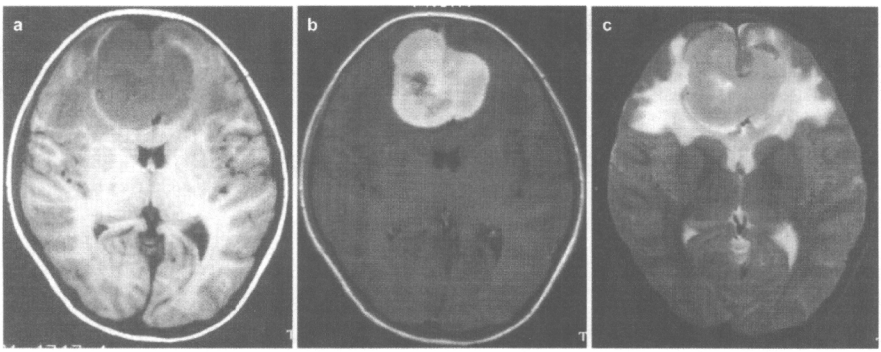

Fig. 1. Magnetic resonance (MR) images obtained at initial presentation. **a** T_1-weighted image showing the midfrontal large tumor. **b** The tumor was homogeneously enhanced by gadolinium. **c** T_2-weighted MR image of the tumor with massive peritumoral brain edema

gadolinium administration. Angiography revealed blood supplies from the cortical branches of the bilateral anterior cerebral arteries (ACAs) and the right anterior falx artery. Based on these findings, the preoperative diagnosis was falx meningioma. Bifrontal craniotomy exposed the very firm, hemorrhagic tumor, which was mostly demarcated from the adjacent brain. The tumor was subtotally removed, leaving the region tightly attached to the bilateral ACAs at the A3 portions. The histopathological diagnosis was MNT.

The postoperative course was uneventful, and the preexisting symptoms caused by increased intracranial pressure resolved immediately. Five months after the initial surgery, gamma knife radiosurgery (GRS), with a maximum dose of 36 Gy and a marginal dose of 18 Gy, was performed for the residual tumor because of its tendency to enlarge (Fig. 2a). The enhanced lesion disappeared post-GRS (Fig. 2b). Three years after the initial GRS, local recurrence was again detected (Fig. 2c). A second GRS, with a maximum dose of 23.5 Gy and a marginal dose of 20 Gy, was performed. The enhanced lesion again disappeared (Fig. 2d). The patient was carefully followed up by MR imaging.

She was admitted to our hospital because of local recurrence of the tumor in February 2009, 12 years after the second GRS. MR imaging detected the irregular tumor, which was isointense with the cortex on both T_1- and T_2-weighted images with heterogeneous enhancement by gadolinium, located in front of the genu of the corpus callosum (Fig. 3a,b). Bifrontal craniotomies exposed the tumor located behind the removal cavity. The tumor consisted of a hard whitish fibrous component, which corresponded to the region treated twice by GRS, and a soft grayish viable component (Fig. 4). Subtotal removal of the tumor was performed, leaving part of the hard component adhered firmly to bilateral ACAs at the A3 portions. Histopathological examination, including reexamination of the specimens obtained at initial surgery, confirmed the recurrence of MNT. Her postoperative course was uneventful and she was discharged without neurological deficit. Postoperative MR imaging showed a residual enhanced tumor in front of the genu of the corpus callosum (Fig. 3c,d).

Pathological findings

The pathological studies from the first surgery revealed MNT. The tumor consisted of small round cells and melanin-containing large cells in a background of dense fibrous stroma (Fig. 5a,b). Small round cells proliferated with moderate to high cellularity. The nuclei incorporated granulated chromatins of moderate density, were round to oval, and appeared isomorphic. The nuclei were clearly demarcated and embedded in sparse, clear cytoplasm. Mitotic activity was low, and no necrosis was detected. Immunostaining was positive for synaptophysin, CD56, neuron-specific enolase (NSE), and neurofilament protein (NFP), and negative for pancytokeratin, HHF-35, glial fibrillary acidic protein (GFAP), olig2, human melanoma black (HMB)-45, S-100 protein, CD99, and WT-1 (Fig. 6). Fluorescence in situ hybridization (FISH) analysis was negative for rearrangement of Ewing sarcoma breakpoint region gene (EWSR). The MIB-1 labeling index was 21%.

The pathological studies from the second surgery revealed recurrent MNT. The tumor consisted of small round cells resembling the initial specimen (Fig. 5c). These cells were arranged in diffuse small clusters or funicular pattern within hyaline fibrous tissue with low cellularity. The nucleus-to-cytoplasm ratio was high, and the nuclei were hyperchromatic with granular chromatin. The mitotic frequency was low and appeared isomorphic. Astroglial cells were also present in some parts. Melanin-containing cells were not evident. The findings of both immunohistochemical and FISH analyses were the same as the initial specimens. The MIB-1 labeling index was 16%.

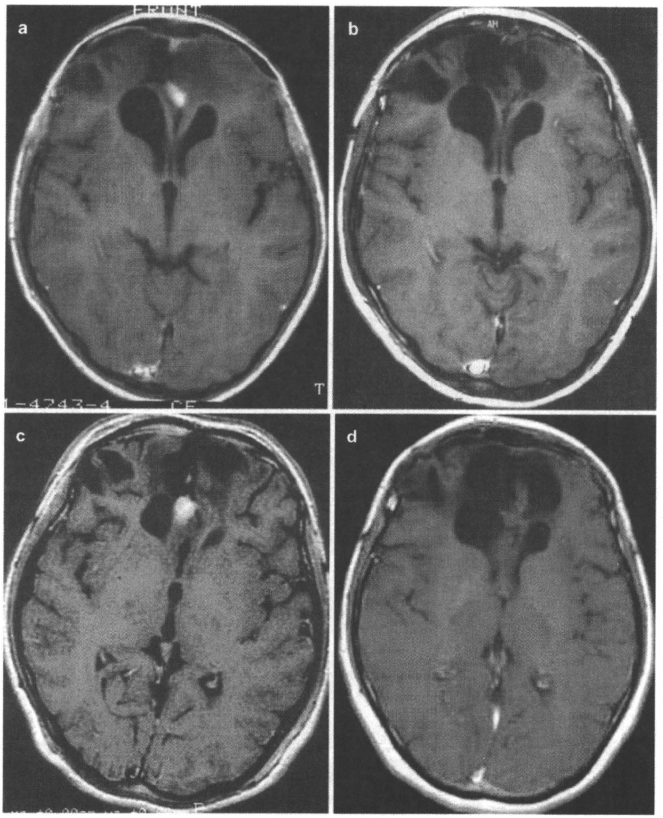

Fig. 2. T_1-weighted MR images with gadolinium obtained during the 15-year follow-up period. **a** Regrowth of the tumor was detected 5 months after initial surgery. **b** Complete remission after first gamma knife radiosurgery (GRS). **c** Local recurrence 3 years after first GRS. **d** Complete remission after second GRS

Discussion

Histologically, MNTs are biphasic tumors characterized by larger polygonal epithelioid cells resembling melanocytes, with variable deposits of melanin, and smaller neuroblast-like round cells in a stroma of fibrous tissue.[1,7,8] Mitotic index is usually low,[9] but malignant cases have a similar histological appearance with increased mitosis, hypercellularity, and focal necrosis.[10] The diagnosis of MNT may be confirmed by immunohistochemical demonstration of multiphenotypic expression for epithelial, melanocytic, and neural markers. Typically, the small round cells express CD56 and synaptophysin, and the melanin-containing large cells express cytokeratin and HMB-45, although the reported findings of immunohistochemical expression seem rather inhomogeneous.[2] Together with the distinctive clinical and histological features, recognition of the multiphenotypic expression of MNT should avoid any serious misdiagnosis.[10] In the present case, the tumor consisted of small round cells and melanin-containing large cells. The immunohistological features were similar to those of previous cases of MNT, with positive staining for the neuroendocrine/neural markers synaptophysin, CD56, NSE, and NFP.

The differential diagnosis of MNT includes other pediatric "small round cell" neoplasms. In this case, immunohistochemical study showed that negative staining of the small round cells for pancytokeratin/HHF-35, olig2/GFAP, HMB-45/S-100 protein, CD99, and WT-1 excluded rhabdomyosarcoma, glioma, malignant melanoma, Ewing sarcoma/primitive neuroectodermal tumor (PNET), and desmoplastic small round cell tumor, respectively. The FISH analysis, negative for EWSR, also supported the exclusion of Ewing sarcoma/PNET. Histological examination of the specimens

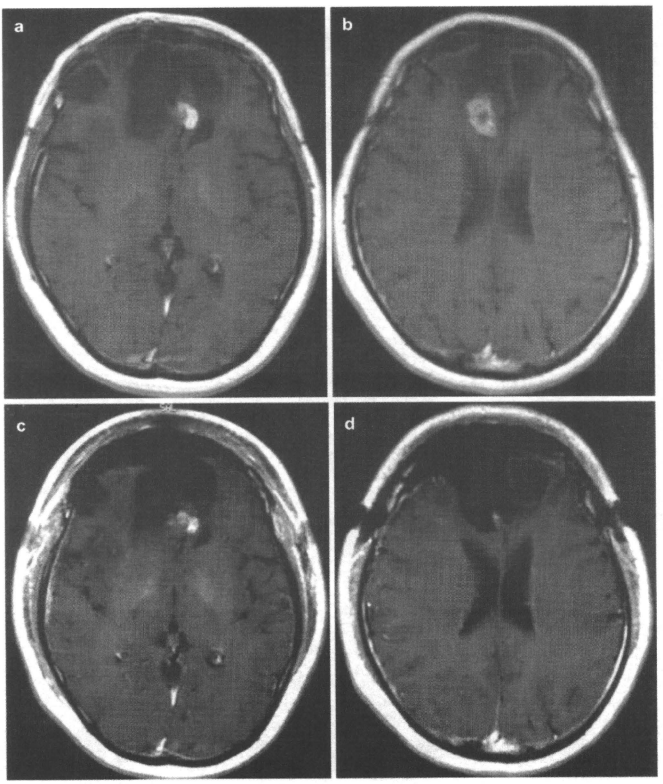

Fig. 3. T_1-weighted MR images with gadolinium before (**a**, **b**) and after (**c**, **d**) second surgery. **a**, **b** Heterogeneously enhanced recurrent tumor located in front of the genu of the corpus callosum. **c**, **d** Residual enhanced lesion observed after subtotal removal of the tumor

obtained at second surgery revealed proliferation of small round cells within the hyaline fibrous stroma, which indicated change after radiation, and the appearance of astroglial cells. The small round cells were similar to those at initial surgery, and the results of the immunohistological/molecular analysis were also similar. These findings indicated that MNT recurred locally and intraaxially after radiotherapy.

Primary MNTs of the brain are rare. Since the first case described in 1957,[11] only 28 MNTs of the brain, including the present case, have been reported (Table 1).[3,12-14] MNTs are regarded as tumors of infancy, with only 8.9% of the affected children aged over 12 months.[2] In contrast, 75% of the patients with MNTs of the brain are aged over 12 months, with mean age 7.3 years (range, 3.5 months to 69 years). All tumors were exclusively located around the midline. The most common sites of origin were the vermis (50.0%) and pineal region (17.9%). The present case is the first originating from the midfrontal region. The midline location of MNTs accords with the widely proposed origin from the neuroectoderm (neural crest). Peripheral MNTs are considered to have a benign clinical course, but MNTs of the brain have a much less favorable prognosis. Fifteen of 23 patients (65.2%) died with a postoperative survival time of just 9 months (range, 3 weeks to 2.5 years), whereas 8 patients were still alive within the observation period of 6 weeks to 16 years. MNTs of the brain tend to spread rapidly throughout the central nervous system. Histological malignancy or systemic metastasis was confirmed in 11 cases (39.3%). However, the biological behavior of MNTs, such as the potential for local recurrence or metastases, cannot be predicted from the clinical or histological features.[10]

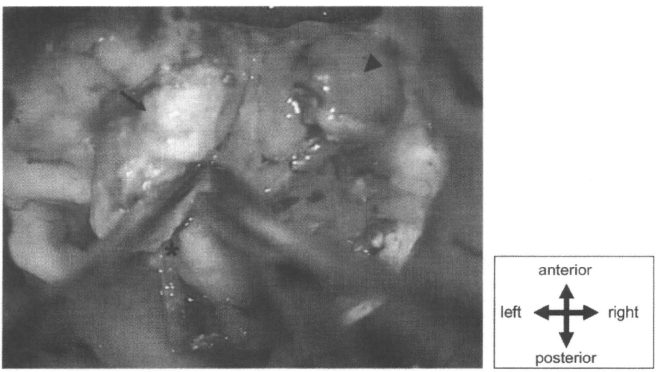

Fig. 4. Intraoperative photograph obtained at the second surgery shows the recurrent tumor consisted of a hard whitish fibrous component (*arrow*), which was firmly adhered to the bilateral anterior cerebral arteries (ACAs) at the A3 portions (*asterisk*), and a soft grayish viable component (*arrowhead*)

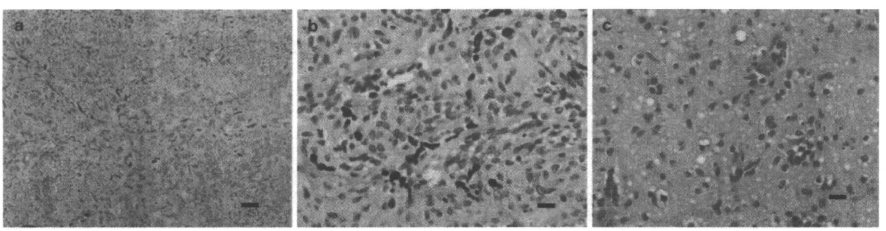

Fig. 5. Micrographs of histological findings obtained at the initial surgery (**a**, **b**) and second surgery (**c**). **a**, **b** Hematoxylin and eosin (H&E) staining shows the biphasic cell population consisting of larger melanin-containing cells and small rounded cells. **c** H&E staining shows small round cells with astroglial cells in a background of organized hyaline fibrous tissue. *Bars* **a** 100 μm; **b**, **c** 25 μm

Table 1. Previously reported cases of melanotic neuroectodermal tumors of brain

Year reported	Age/sex	Location	Survival
1957	5 years/M	Vermis	D, 4 months
1962	2.5 years/M	Vermis	D, 3 weeks
1964	8 years/nd	Vermis	D, 30 months
1966	nd/nd	Vermis (4 cases)	D, nd
1973	12 months/M	Cerebellum, pineal region	D, 5 weeks
1973	3 years/M	Vermis	D, 2 months
1974	3.5 months/F	Third ventricle	D, 18 months
1976	21 years/M	Vermis	A, >9 months
1978	4 years/M	Vermis	A, >6 weeks
1979	4 months/F	Middle fossa	nd
1979	17 months/M	Vermis	D, 19 months
1980	6 months/M	Mesencephalon	D, 2 months
1981	14 years/M	Sellar region	nd
1983	7 years/M	Cerebellum	nd
1983	3 years/M	Cerebellum	nd
1986	69 years/M	Medulla oblongata	A, >7 months
1988	4 months/nd	Pineal gland	A, >30 months
1989	4 years/F	Pineal gland	D, 12 months
1989	4 years/M	Vermis, cerebellar hemisphere	nd
1991	21 months/M	Vermis	A, >6 years
1992	3 years/M	Vermis	D, 3 weeks
1993	9 years/F	Brain	A, >20 months
1998	12 months/M	Pineal gland	D, 10 months
2001	23 months/M	Pineal gland	A, >2 years
Present case	11 years/F	Frontal lobe	A, >16 years

M, male; F, female; nd, no data available; A, alive; D, dead
Source: References 3, 12, 13, 14

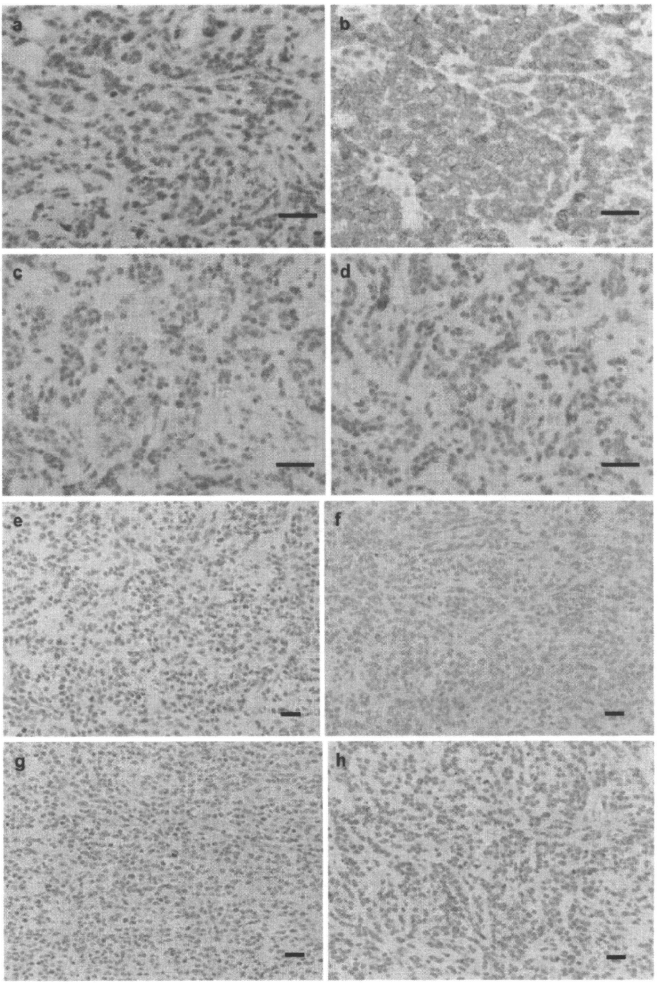

Fig. 6. Immunohistochemical staining of specimens obtained from the initial surgery. Tumor cells showed positive staining for synaptophysin (**a**), CD56 (**b**), neuron-specific enolase (NSE) (**c**), and neurofilament protein (NFP) (**d**), and negative staining for glial fibrillary acidic protein GFAP (**e**), olig2 (**f**), CD99 (**g**), and WT-1 (**h**). *Bars* **a–h** 50 μm

The primary surgical approach achieving total excision is the preferred procedure and is curative in most cases of MNT. However, MNTs of the brain are often difficult to remove totally, because of their invasive tendency and the midline location, which results in involvement of the adjacent critical anatomical structures. Patients with MNT not amenable to surgical management may receive radiotherapy and/or chemotherapy.[15] Some patients were treated by radiotherapy, but the efficacy was not evident. Our treatment included GRS twice because of local recurrence after subtotal tumor resection. GRS was effective in obtaining complete remission of the tumor, but local recurrence was detected 3 and 12 years after each GRS.

The present MNT of the brain was unusual in the location in the midfrontal region and in its recurrence more than 10 years after the combined treatment of surgery and

radiotherapy. This case suggests that MNTs not treated by complete resection require long-term follow up, even if complete remission was achieved after adjuvant therapy.

References

1. Barrett AW, Morgan M, Ramsay AD, et al (2002) A clinicopathologic and immunohistochemical analysis of melanotic neuroectodermal tumor of infancy. Oral Surg Oral Med Oral Pathol Oral Radiol Endod 93:688–698
2. Kruse-Losler B, Gaertner C, Burger H, et al (2006) Melanotic neuroectodermal tumor of infancy: systematic review of the literature and presentation of a case. Oral Surg Oral Med Oral Pathol Oral Radiol Endod 102:204–216
3. Rickert CH, Probst-Cousin S, Blasius S, et al (1998) Melanotic progonoma of the brain: a case report and review. Childs Nerv Syst 14:389–393
4. Dammann O, Hagel C, Allers B, et al (1995) Malignant melanotic neuroectodermal tumor of infancy. Childs Nerv Syst 11:186–188
5. Nagase M, Ueda K, Fukushima M, et al (1983) Recurrent melanotic neuroectodermal tumour of infancy. Case report and survey of 16 cases. J Maxillofac Surg 11:131–136
6. Woessmann W, Neugebauer M, Gossen R, et al (2003) Successful chemotherapy for melanotic neuroectodermal tumor of infancy in a baby. Med Pediatr Oncol 40:198–199
7. Mosby EL, Lowe MW, Cobb CM, et al (1992) Melanotic neuroectodermal tumor of infancy: review of the literature and report of a case. J Oral Maxillofac Surg 50:886–894
8. Cutler LS, Chaudhry AP, Topazian R (1981) Melanotic neuroectodermal tumor of infancy: an ultrastructural study, literature review, and reevaluation. Cancer (Phila) 48:257–270
9. Selim H, Shaheen S, Barakat K, et al (2008) Melanotic neuroectodermal tumor of infancy: review of literature and case report. J Pediatr Surg 43:E25–E29
10. Kapadia SB, Frisman DM, Hitchcock CL, et al (1993) Melanotic neuroectodermal tumor of infancy. Clinicopathological, immunohistochemical, and flow cytometric study. Am J Surg Pathol 17:566–573
11. Stowens D (1957) A pigmented tumor of infancy: the melanotic progonoma. J Pathol Bacteriol 73:43–51
12. Ishida Y, Kawarai M, Tanaka T, et al (1979) Medulloblastoma-like tumor of the cerebellum with melanin formation (melanotic medulloblastoma) (in Japanese). No To Shinkei (Brain Nerve) 31: 813–821
13. Mirich DR, Blaser SI, Harwood-Nash DC, et al (1991) Melanotic neuroectodermal tumor of infancy: clinical, radiologic, and pathologic findings in five cases. AJNR Am J Neuroradiol 12:689–697
14. Gorhan C, Soto-Ares G, Ruchoux MM, et al (2001) Melanotic neuroectodermal tumour of the pineal region. Neuroradiology 43:944–947
15. Shaia WT, Dinardo LJ, Underhill TE, et al (2002) Recurrent melanotic neuroectodermal tumor of infancy. Am J Otolaryngol 23:249–252

Tohoku J. Exp. Med., 2010, 221, 257-264

Convection-Enhanced Delivery of a Synthetic Retinoid Am80, Loaded into Polymeric Micelles, Prolongs the Survival of Rats Bearing Intracranial Glioblastoma Xenografts

Michiko Yokosawa,[1] Yukihiko Sonoda,[1] Shin-ichiro Sugiyama,[1] Ryuta Saito,[1] Yoji Yamashita,[1] Masamichi Nishihara,[2] Taku Satoh,[2] Toshihiro Kumabe,[1] Masayuki Yokoyama[2] and Teiji Tominaga[1]

[1]Department of Neurosurgery, Tohoku University Graduate School of Medicine, Sendai, Japan
[2]Yokoyama Nano-medical Polymers Project, Kanagawa Academy of Science and Technology, Kawasaki, Japan

Prognosis for the patients with glioblastoma, the most common malignant brain tumor, remains dismal. A major barrier to progress in treatment of glioblastoma is the relative inaccessibility of tumors to chemotherapeutic agents. Convection-enhanced delivery (CED) is a direct intracranial drug infusion technique to deliver chemotherapeutic agents to the central nervous system, circumventing the blood-brain barrier and reducing systemic side effects. CED can provide wider distribution of infused agents compared to simple diffusion. We have reported that CED of a polymeric micelle carrier system could yield a clinically relevant distribution of encapsulated agents in the rat brain. Our aim was to evaluate the efficacy of CED of polymeric micellar Am80, a synthetic agonist with high affinity to nuclear retinoic acid receptor, in a rat model of glioblastoma xenografts. We also used systemic administration of temozolomide, a DNA-alkylating agent, which has been established as the standard of care for newly diagnosed malignant glioma. U87MG human glioma cells were injected into the cerebral hemisphere of nude rats. Rats bearing U87MG xenografts were treated with CED of micellar Am80 (2.4 mg/m^2) on day 7 after tumor implantation. Temozolomide (200 mg/m^2/day) was intraperitoneally administered daily for 5 days, starting on day 7 after tumor implantation. CED of micellar Am80 provided significantly longer survival than the control. The combination of CED of micellar Am80 and systemic administration of temozolomide provided significantly longer survival than single treatment. In conclusion, temozolomide combined with CED of micellar Am80 may be a promising method for the treatment of malignant gliomas.

Keywords: Am80; glioblastoma; convection-enhanced delivery; temozolomide; polymeric micelle
Tohoku J. Exp. Med., 2010, **221** (4), 257-264.

Glioblastoma is the most common primary malignant brain tumor in adults. Despite therapeutic advances, the median survival continues to be approximately 12 months. Therefore, a new therapeutic approach is required.

Convection-enhanced delivery (CED) is a relatively new method that might overcome the problems posed by the requirements of local drug delivery (Bobo et al. 1994). CED uses a pressure gradient established at the tip of an infusion catheter to create bulk-flow that pushes the drug through the interstitial spaces. CED of therapeutic agents bypasses the blood-brain barrier, delivers high concentrations of therapeutic agents to the target site, and minimizes systemic exposure, thus resulting in fewer side effects. CED has been used to deliver many antineoplastic agents in animal studies with promising outcomes (Bruce et al. 2000; Degen et al. 2003; Vogelbaum 2007). However, CED of free drugs has various problems including rapid clearance from the tumor interstitium, so no selective accumulation in the targeted tissue can be achieved (Kunwar et al. 2007). We considered that it was necessary to develop a new pharmaceutical composition comprising an effective CED agent.

Drug carrier systems offer the advantage of sustained drug release as well as targeting of specific sites. Liposomes have been used as drug carriers in combination with CED (Saito et al. 2004, 2006a, 2006b; Noble et al. 2006; Yamashita et al. 2007; Kikuchi et al. 2008). Recently, we demonstrated the therapeutic efficacy of a newer type of drug carrier system, polymeric micellar doxorubicin, which was infused by CED in rat brain tumor models (Inoue et al. 2009). Polymeric micelles are an assembly of synthetic polymers, which typically block copolymers with both hydrophobic and hydrophilic properties. Polymeric micelle

Received March 10, 2010; revision accepted for publication June 17, 2010. doi:10.1620/tjem.221.257
Correspondence: Yukihiko Sonoda, M.D. Ph.D., Department of Neurosurgery, Tohoku University Graduate School of Medicine, 1-1, Seiryo-machi, Aoba-ku, Sendai, 980-8574, Japan.
e-mail: sono@nsg.med.tohoku.ac.jp

carrier systems were first studied for targeting solid tumors by intravenous injection (Yokoyama et al. 1990, 1999). Polymeric micelle carrier systems are electrically neutral and have the so-called stealth property that evades rapid clearance by the reticuloendothelial system. Consequently, systemic administration of polymeric micelle systems is effective against solid tumors because of the enhanced permeability and retention effect, which depends on the hyperpermeable vasculature and the absence of effective lymphatic drainage that prevents efficient clearance of macromolecules in the solid tumor tissues (Greish 2007). Various micelle-encapsulated cytotoxic agents are currently undergoing clinical evaluation for systemic administration, including doxorubicin (Tsukioka et al. 2002), paclitaxel (Hamaguchi et al. 2007), cisplatin (Uchino et al. 2005), and a camptothecin derivative SN-38 (Koizumi et al. 2006).

All-trans retinoic acid (ATRA) and other retinoids are reported to inhibit the growth rate of various malignancies including acute polymyelocytic leukemia, lung cancer, and glioblastoma both in vivo and in vitro (Flynn et al. 1983; Yung et al. 1996; Jaeckle et al. 2003). ATRA induces cell differentiation, cell cycle arrest, apoptotic cell death, and interleukin 6/interleukin 6 receptor downregulation in vitro. Retinoid effects are mediated through the interaction with two types of nuclear receptors, retinoic acid receptor (RAR) and retinoid X receptor (RXR), each of which has three subtypes (-α, -β, and -γ). ATRA is one of the most clinically effective retinoids; nevertheless, high rates of adverse effects have been reported such as exanthesis, fever, and xeroderma (Delva et al. 1993). The adverse effect on the skin is due to the large number of RAR-γ receptors distributed in the skin. The definition of retinoids has been expanded to include molecules that bind to RARs and RXRs, regardless of the similarity in molecular structure to ATRA. Am80 is such a synthetic retinoid with strong binding affinity to the nuclear receptors, but has a very different chemical structure to ATRA (Tobita et al. 1997). Am80 is a RAR-α/β-selective retinoid that does not activate RAR-γ and RXRs, so it may not cause adverse effects. Am80 is a promising candidate for CED infusion because glioma cells have extensive expression of RAR-α/β (Chattopadhyay et al. 2001; Costa et al. 2001). Alkylating agents and retinoids are among the chemotherapeutic agents that have shown activity against gliomas, either individually or in combination. Temozolomide and 13-cis-retinoic acid have also shown activity against recurrent gliomas in phase II clinical trials (Yung et al. 1996; Wismeth et al. 2004).

In the present study, we evaluated the efficacy of CED administration of micellar Am80 and/or systemic administration of temozolomide in the intracranial xenograft model.

Methods

Preparation of Agents

Am80 was kindly provided by Dr. Koichi Shudo of the Research Foundation Itsuu Laboratory (Tokyo, Japan). Temozolomide was provided by Schering-Plough K.K. (Osaka, Japan) and was dissolved in a solution of 0.1% dimethyl sulfoxide (Sigma Chemical Co., St. Louis, MO) in 0.9% NaCl solution.

Am80 was incorporated into a polymeric micelle formed from poly(ethylene glycol)-β-poly(benzyl aspartate) block copolymer. The polymer synthesis, Am80 incorporation into the polymeric micelle carrier, and characterization of the carrier system were as previously described (Satoh et al. 2009). Briefly, the block copolymer and Am80 were dissolved in tetrahydrofuran, and the obtained solution was subjected to solvent evaporation. Water was added to the dried residue, followed by sonication. The micelle solution was centrifuged to remove any insoluble precipitate (3,900 rpm, 10 min, 20°C) and then filtered through a Millex 0.22 μm PVDF filter (Millipore Corp, Billerica, MA). The composition of the block copolymer was as follows. The mean molecular weight of the poly(ethylene glycol) chain was 5,200, and the mean unit number of the poly(aspartic acid) chain was 24. Hydrophobic benzyl ester was formed at 83 mol% of the aspartic acid residue. Therefore, the mean molecular weight of the poly(aspartate) chain (83% benzyl aspartate residues and 17% aspartic acid residues) was 4600. In addition, N,N-dimethyloctadecylamine was added as a hydrophobic amine with Am80 at a molar ratio of 1:1 in the micelle preparation step. The drug content by weight in the polymeric micelle was 14%.

Tumor Cell Line

The established human glioblastoma cell line U87MG was obtained from the American Type Culture Collection (Rockville, MD). Cells were maintained as monolayers in a complete medium consisting of Eagle's minimal essential medium supplemented with 10% fetal calf serum, non-essential amino acids, and 100 U/ml penicillin G. Cells were cultured at 37°C in a humidified atmosphere consisting of 95% air and 5% CO_2.

Cell Viability Assay

The cell viability of U87MG cell lines treated with Am80 and temozolomide was assessed using the MTS assay (CellTiter96 Aqueous One Solution Cell Proliferation Assay; Promega Corp, Madison, WI). MTS, (3-(4,5-dimethylthiazol-2-yl)-5-(3-carboxymethoxyphenyl)-2-(4-sulfophenyl)-2H-tetrazolium), was reduced by living cells in the presence of phenazine methosulfate (PMS) to yield a purple formazan product that could be assayed colorimetrically. Cells were seeded at 750 cells per well in 75 μl of medium in 96-well flat-bottom plates and grown overnight at 37°C in an incubator. Temozolomide was used at 100 μM as described previously (Das et al. 2005). After exposure to Am80 (0, 50, 100, 200, or 500 μM), temozolomide (100 μM), and a combination of the two agents (100 μM Am80 + 100 μM temozolomide) for 24 hours, the plates were assayed with a microplate reader (Softmax Pro; Molecular Devices Corp, Sunnyvale, CA). Results were compared using one-way analysis of variance (ANOVA) with Tukey's Multiple Comparison test at a 95% confidence interval.

Western Blot Analysis

On the day before treatment, 1×10^6 cells per dish were seeded. After 24 hours incubation, cells were treated with Am80 (100 μM), temozolomide (100 μM), or a combination of both agents. Cells were collected 24 hours and 48 hours after the treatment. Protein was extracted from these cells with a mammalian protein extraction reagent (M-PER; Thermo Scientific, Rochester, NY). Samples were then prepared in sample buffer (Novex; Invitrogen, Carlsbad, CA) and

heated to 94°C for 5 minutes. Samples were then subjected to electrophoresis on 10% polyacrylamide gels (or 16% gels only for cleaved caspase-3), and then blotted onto polyvinylidene fluoride membranes (PDVF) (Invitrogen). PDVF were then incubated overnight with primary antibody against phospho-mitogen-activated protein kinase (phospho-MAPK) (Cell Signaling Technology, Cambridge, MA; 1:200), phospho-Akt (Cell Signaling Technology; 1:200), cleaved caspase-3 (Cell Signaling Technology; 1:500), cleaved caspase-9 (Cell Signaling Technology; 1:500), and β-actin (Santa Cruz Technology, Santa Cruz, CA; 1:1000). The residue targets for each phospho-specific antibody were p-MAPK (Thr202/Tyr204) and p-Akt (Thr308). The membranes were washed 3 times in Tris-buffered saline containing Tween 20, then incubated with secondary antibody for 60 minutes and subsequently washed. The blot was visualized with the ECL Plus Western Blotting Detection System (GE Healthcare Bioscience, Little Chalfont, Buckinghamshire, UK).

Animals

Male Sprague–Dawley rats weighing approximately 200 g were obtained from Charles-River Japan, Inc. (Yokohama, Kanagawa, Japan). Seven-week-old male Fischer 344/NJcl-rnu/rnu (nude) rats were purchased from CLEA Japan, Inc. (Tokyo, Japan). All protocols used in the animal studies were approved by the Institute for Animal Experimentation of Tohoku University Graduate School of Medicine.

Intracranial Tumor Implantation

U87MG cells were harvested by trypsinization, washed once with Hanks balanced salt solution without Ca^{2+} and Mg^{2+} (HBSS), and resuspended in HBSS for implantation. A cell suspension containing 5×10^5 cells per 10 μl of HBSS was used for implantation into the striatum of rat brains. Rats were placed in a small animal stereotactic frame (Narishige Manufacturing Co., Ltd., Japan) under deep halothane anesthesia. A sagittal incision was made through the skin to expose the cranium, and a burr hole was made in the skull at 0.5 mm anterior and 3 mm lateral from the bregma using a small dental drill. Cell suspension (5 μl) was injected at a depth of 4.5 mm from the brain surface. After a wait of 2 minutes, another 5 μl was injected at a depth of 4 mm. After a final wait of 2 minutes, the needle was removed, and the wound was closed with sutures.

CED

CED of micellar Am80, free Am80, or PBS was performed with a volume of 20 μl as described previously (Saito et al. 2006b). The infusion system consisted of a reflux free step-design infusion cannula connected to a loading line (containing micellar Am80, free Am80, or PBS) and an olive oil infusion line. A 1-ml syringe (filled with olive oil) mounted onto a micro-infusion pump (BeeHive; Bioanalytical Systems, West Lafayette, IN) regulated the flow of fluid through the system. On the basis of the chosen coordinates, the infusion cannula was mounted onto stereotactic holders and guided to the target region of the brain through the same burr holes made in the skull at tumor implantation. The following ascending infusion rates were applied for the 20-μl infusion: 0.2 μl/min for 15 minutes, 0.5 μl/min for 10 minutes, and 0.8 μl/min for 15 minutes.

Evaluation of Micellar Am80 Toxicity

Sprague–Dawley rats (3 rats in each group) received a single 20 μl CED infusion of micellar Am80. To ensure the safety of micellar Am80, the starting dose of 2.4 mg/m^2, available highest dose of micellar Am80, was chosen. The dose of 1.2 mg/m^2 and 0.6 mg/m^2 were also evaluated. Rats were monitored daily for survival, weekly for weight, and for general health (alertness, grooming, feeding, excreta, skin, fur, mucous membrane conditions, ambulation, breathing, and posture). The rats were euthanized 6 weeks after the CED treatment, and their brains were removed, fixed, sectioned (5 μm), and stained with hematoxylin and eosin and examined using a stereoscopic microscope (SZX7; Olympus Corp, Tokyo, Japan) and a light microscope (ECLIPSE 80i; Nikon Corp, Tokyo, Japan).

Survival Studies

Thirty rats implanted with U87MG tumor cells were randomly assigned to 6 groups of 5 rats: 1) a control group treated with CED of PBS (20 μl solution), 2) a group that underwent systemic treatment with temozolomide (200 mg/m^2/day), 3) a group treated with CED of free Am80 (2.4 mg/m^2 Am80 in a 20 μl solution), 4) a group treated with CED of micellar Am80 (2.4 mg/m^2 Am80 in a 20 μl solution), 5) a group that underwent systemic treatment with micellar Am80 (2.4 mg/m^2 Am80 in a 20 μl solution) and systemic treatment with temozolomide (200 mg/m^2/day), and 6) a group treated with CED of Am80 (2.4 mg/m^2 Am80 in a 20 μl solution) and systemic treatment with temozolomide (200 mg/m^2/day). CED infusion of free Am80 or micellar Am80 was performed on day 7 after tumor implantation. Systemic treatment with temozolomide consisted of a dose of 200 mg/m^2/day in a solution of 10% dimethyl sulfoxide in 0.9% NaCl solution for a total volume of 90 ml/m^2, which was intraperitoneally administered daily for 5 days, starting on day 7 after tumor implantation. Systemic treatment of micellar Am80 was performed by injection through the tail vein 7 days after tumor implantation. Rats were monitored daily for survival and general health. Survival rates in the treatment groups were compared using a log-rank test. Estimated survival was expressed as a Kaplan-Meier curve.

Terminal Deoxynucleotidyl Transferase dUTP Nick End Labeling (TUNEL) Staining

Eight rats implanted with U87MG tumor cells were randomly assigned to 4 groups of 2 rats: 1) a control group, 2) a group treated with CED of micellar Am80, 3) a group treated with systemic temozolomide, and 4) a group treated with CED of micellar Am80 and systemic temozolomide. Paraffin sections made from the brains of 2 rats from each group euthanized 12 days after tumor implantation were examined for apoptosis. The sections were deparaffinized followed by incubation with NaN_3 and H_2O_2 in PBS with 0.3% Triton-X for 20 minutes at room temperature. Then, the slides were washed 3 times with PBS. After incubation with terminal deoxynucleotidyl transferase (TdT) buffer (TdT, Recombinant; Invitrogen) for 15 minutes at room temperature, a mixture of TdT (2.5 μl) (Invitrogen), biotinylated 16-dUTP (6 μl) (Roche Diagnostics, Mannheim, Germany), and TdT buffer (100 μl) was added to each slide for 60 minutes at 37°C. Then, the slides were washed 2 times with TB buffer (6 mM sodium citrate, 60 mM NaCl) and blocked by incubation in 2% bovine serum albumin in PBS for 15 minutes at room temperature, followed by washing 3 times after blocking and incubation in an avidin-biotin peroxidase complex (ABC) solution (VECTASTAIN Elite ABC Standard Kit; Vector Laboratories Inc., Burlingame, CA) in PBS for 30 minutes at room temperature. The slides were twice washed with 0.175 M sodium acetate for 10 minutes and then reacted with 3′ 3-diaminobenzidine hydrochloride for appropriate times. Counterstaining was performed with methyl green solution.

Results

Enhanced Cytotoxic Effects of Am80 and Temozolomide In Vitro

Am80 significantly reduced the viability of U87MG cells in a dose-dependent manner through U87MG cells seeded in a 96-well flat-bottom plate and treated after 24 hours, then incubated for 2, 4, and 6 days (Fig. 1A). Inhibition of cell growth was high at 4 and 6 days after treatment. The 50% inhibition concentration (IC50) of Am80 was 123 μM. In combination with temozolomide, Am80 was used at 100 μM, approximate IC50 concentrations. Am80 combined with temozolomide achieved additional reduction in cell viability (Fig. 1B). Expression levels of phospho-Akt, phospho-MAPK, cleaved caspase-3, cleaved caspase-9, and β-actin were evaluated by western blot analysis using antibodies that detect only the phosphorylated forms of these proteins (Fig. 2). Treatment with Am80 or temozolomide showed a modest decrease in the expression of phospho-Akt protein, but treatment with Am80 and temozolomide further decreased the expression. Expression of phospho-MAPK was strongly suppressed in cells treated with Am80 or temozolomide, and the suppression effect was sustained in cells treated with these in combination. Western blot analyses for cleaved caspase-3 and cleaved caspase-9 indicated the activation of caspase-3 and caspase-9, respectively, in U87MG cells treated with temozolomide, Am80, or the combination of temozolomide and Am80. Similar levels of activation of both caspases were observed in the U87MG cells treated with temozolomide alone and Am80 alone. The combination of Am80 and temozolomide enhanced activation of both caspases. The molecular events occurring during synergistic induction of cell death due to temozolomide and Am80 were characterized in U87MG cells.

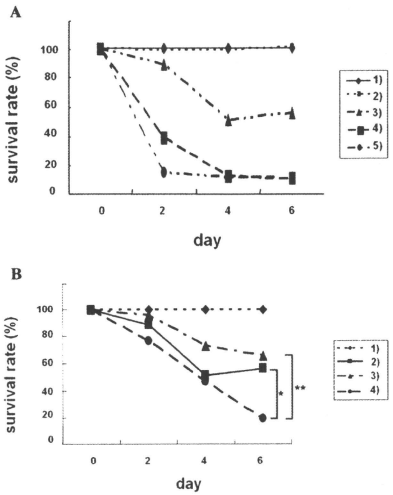

Fig. 1. Effects of Am80 and its combination with temozolomide on the viability of U87MG cells.
Shown are the effects of Am80 alone (A) and its combination with temozolomide (B) on the viability of U87MG cells, as determined by MTS assay. U87MG cells were seeded in a 96-well flat-bottom plate and incubated for 24 hours, then treated for 2, 4, and 6 days. Fig. 1A shows the dose-response effects of Am80: 1) 0 μM, 2) 50 μM, 3) 100 μM, 4) 200 μM, and 5) 500 μM. Fig. 1B shows the effects of 1) control, 2) 100 μM Am80, 3) 100 μM TMZ, and 4) 100 μM Am80 + 100 μM TMZ. Significant difference between Am80 treated cells and Am80 + TMZ treated cells was indicated with * ($p < 0.001$) and significant difference between TMZ treated cells and Am80 + TMZ treated cells was indicated by ** ($p < 0.001$).

Toxicity of Am80 in Normal Brain Parenchyma

No dose-limiting toxicity was found at 0.6, 1.2, or 2.4 mg/m^2. Animals that received CED of micellar Am80 at 2.4 mg/m^2 or less showed evidence of minor tissue damage at the site of the infusion cannula in the striatum, but no other apparent toxicity (Fig. 3).

Efficacy of Combined Micellar Am80 and Temozolomide in U87MG Brain Tumor Xenograft In Vivo

All rats from the control group had to be euthanized because of tumor progression between 12 to 16 days after implantation. Single treatment with CED of free Am80 showed no improvement in survival. In contrast, CED of micellar Am80 provided significantly longer survival (p = 0.019, log-rank test). Furthermore, the combination treatment of CED of micellar Am80 and systemic treatment of temozolomide provided significantly longer survival than the single treatment (p = 0.0027 compared with the CED of micellar Am80 group, p = 0.0018 compared with the temozolomide group). However, the combination of systemic administration of micellar Am80 and temozolomide did not achieve longer survival than systemic temozolomide alone (Fig. 4).

Detection of Apoptotic Cell Death after Treatment

TUNEL staining was performed on brain slices of rats from each group euthanized 6 days after treatment had started. Tumors from rats treated with CED of micellar Am80 and temozolomide exhibited decreased tumor density and increased number of TUNEL-positive cells compared with those from animals treated with only agent or control animals (Fig. 5).

Discussion

In the present study, we found that the CED of micellar Am80 provided long survival for rats bearing U87MG xenografts. We previously reported that micellar agents infused by CED were extensively distributed in normal rat

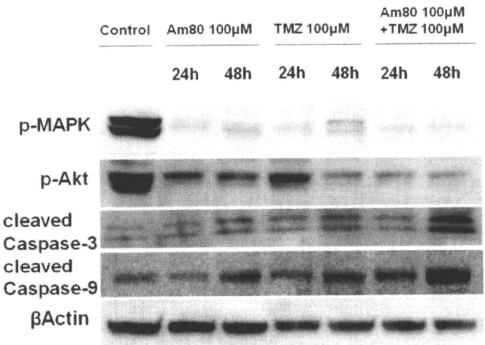

Fig. 2. Western blotting analysis for phospho-Akt, phospho-MAPK, cleaved caspase-3 and -9, and β-actin. The data shown are representative of three experiments.

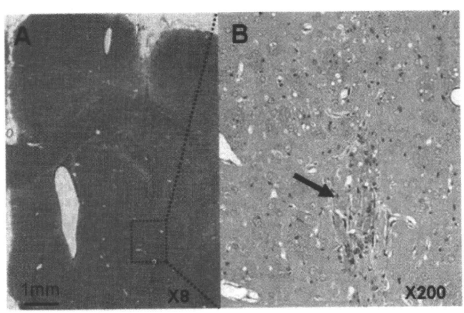

Fig. 3. Toxicity evaluation of micellar Am80 after CED infusion into the brain striatum of wild-type rats. There was only a slight cannulation scar; an arrow indicates small fibrous tissues with inflammation. No damage was induced to the infused hemisphere in any rats. Hematoxylin and eosin stain, original magnification × 8 in a stereoscopic microscope (A) and × 200 in a light microscope (B).

brain (Inoue et al. 2009). We also reported that micellar agents were distributed over almost the entire tumor area, including tumor margins, in rat brain tumor models (Inoue et al. 2009). The distribution of agents infused by CED in the rat brain is significantly increased if the infusate is more hydrophilic, which implies less tissue affinity (Saito et al. 2004, 2006b; MacKay et al. 2005; Yamashita et al. 2007). Furthermore, polyethylene glycol encapsulation provides steric stabilization, reduces surface charge, and achieves better distribution (Inoue et al. 2009). In the present study, the poorer brain/tumor tissue distribution caused by Am80 hydrophobicity might be overcome by polymeric micelle carrier system.

On the other hand, micellar Am80 administered intravenously did not contribute to long survival for rats bearing U87MG xenografts, despite the fact that micellar agents have been shown to accumulate around tumor vessels and effectively pass through brain tumor vessels (Kuroda et al. 2009). Although this study lacks monitoring or confirmation of infusate, it is speculated that micellar Am80 administered systemically could not sufficiently penetrate into the hypovascular central area of implanted tumor with three-dimensional cellular structures, in which the diffusion of infusate was restricted. Development of monitoring of the distribution of infusate is required to gain a deeper appreciation of micellar Am80.

Several chemotherapeutic agents delivered locally using CED, including 1,3-bis(chloroethyl)-1-nitrosourea (Bruce et al. 2000), gemcitabine, and carboplatin (Degen et al. 2003), prolonged survival of rats bearing U87MG xeno-

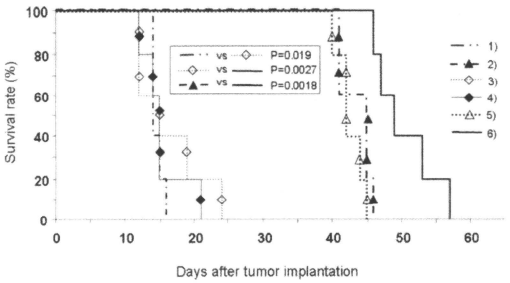

Fig. 4. Survival of treated animals bearing intracranial glioblastoma xenografts.
Survival of treated animals is expressed as a Kaplan-Meier curve (5 rats per each group). Rats bearing intracranial glioblastoma xenografts were treated with 1) vehicle (control), 2) systemic temozolomide (200 mg/m^2/day), 3) CED of the free Am80 (2.4 mg/m^2), 4) CED of micellar Am80 (2.4 mg/m^2), 5) combination of systemic treatment of micellar Am80 (2.4 mg/m^2) and temozolomide (200 mg/m^2/day), and 6) combination of CED of micellar Am80 (2.4 mg/m^2) and systemic temozolomide (200 mg/m^2/day). p-Values were obtained using a log-rank test.

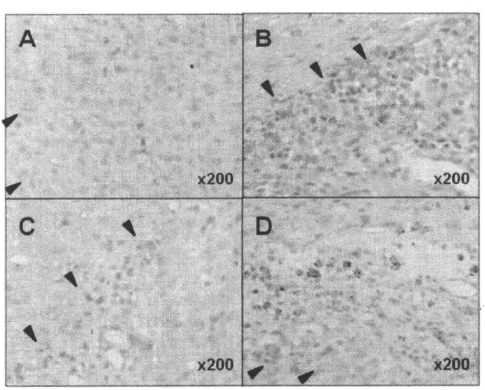

Fig. 5. Histological estimation with TUNEL staining. Brain slices of rats from each group were examined 12 days after tumor implantation. TUNEL-positive cells are stained brown. Arrowheads indicate the margin of xenografts. Counterstaining with methyl green, original magnification × 200. A: control group, B: group treated with CED of micellar Am80, C: group treated with systemic temozolomide, D: group treated with CED of micellar Am80 and systemic temozolomide.

grafts. However, some of these agents applied locally to the cerebrospinal fluid have long-term side effects including leukoencephalopathy and brain atrophy (Shapiro and Young 1984). Ideally, agents for CED administration into brain tumors would show the highest possible therapeutic ratio against tumor cells over normal cells. Retinoids such as Am80 show selective toxicity against neoplastic transformed cells, so they represent an excellent candidate for local delivery (Schneider et al. 2000). In our study, the toxicity of Am80 against normal brain cells was minimal, even with enhanced delivery. These results suggest that CED-delivered Am80 may be a viable therapeutic option (Chattopadhyay et al. 2001).

The most important function of the carrier is the inhibition of rapid drug absorption by cells at the injection site, since the agent cannot be distributed over a large volume of tissue in the presence of rapid absorption. Sustained drug release is needed for effective inhibition of rapid drug absorption by cells. In this study, we prepared polymeric micelles containing Am80, which were observed to sustain

the release of Am80 in vitro more than that of free Am80 (Satoh et al. 2009). For this reason, CED of this micelle was more effective than that of the free agent.

We chose temozolomide as a drug in combination with Am80 because the use of temozolomide is already clinically established for glioma therapy. The strategy for induction of differentiation followed by activation of apoptosis has been highly promising in cancer therapy. We found that Am80 and/or temozolomide treatment down-regulated cell growth signaling, p-MAPK. Activation of Akt is a major event in the development of glioblastoma, and high levels of Akt were frequently expressed in glioblastoma (Sonoda et al. 2001; Choe et al. 2003). Phosphorylation of Akt results in activation of Akt kinase activity, which has the potential to deregulate the cell cycle and suppress apoptosis. The present study demonstrated that treatment of U87MG xenografts with Am80 and temozolomide down-regulated phospho-Akt and activated cleaved caspase-3 and -9, indicating activation of the caspase cascade for apoptosis. In the survival study, CED of micellar Am80 individually or in combination with temozolomide improved the therapeutic outcome in the human glioblastoma model.

Agents such as temozolomide combined with CED administration of micellar Am80 may be promising for the treatment of malignant gliomas.

References

Bobo, R.H., Laske, D.W., Akbasak, A., Morrison, P.F., Dedrick, R.L. & Oldfield, E.H. (1994) Convection-enhanced delivery of macromolecules in the brain. *Proc. Natl. Acad. Sci. USA*, **91**, 2076-2080.

Bruce, J.N., Falavigna, A., Johnson, J.P., Hall, J.S., Birch, B.D., Yoon, J.T., Wu, E.X., Fine, R.L. & Parsa, A.T. (2000) Intracerebral clysis in a rat glioma model. *Neurosurgery*, **46**, 683-691.

Chattopadhyay, N., Butters, R.R. & Brown, E.M. (2001) Agonists of the retinoic acid- and retinoid X-receptors inhibit hepatocyte growth factor secretion and expression in U87 human astrocytoma cells. *Brain Res. Mol. Brain Res.*, **87**, 100-108.

Choe, G., Horvath, S., Cloughesy, T.F., Crosby, K., Seligson, D., Palotie, A., Inge, L., Smith, B.L., Sawyers, C.L. & Mischel, P.S. (2003) Analysis of the phosphatidylinositol 3′-kinase signaling pathway in glioblastoma patients in vivo. *Cancer Res.*, **63**, 2742-2746.

Costa, S.L., Paillaud, E., Fages, C., Rochette-Egly, C., Plassat, J.L., Jouault, H., Perzelova, A. & Tardy, M. (2001) Effects of a novel synthetic retinoid on malignant glioma in vitro: inhibition of cell proliferation, induction of apoptosis and differentiation. *Eur. J. Cancer*, **37**, 520-530.

Das, A., Banik, N.L., Patel, S.J. & Ray, S.K. (2004) Dexamethasone protected human glioblastoma U87MG cells from temozolomide induced apoptosis by maintaining Bax:Bcl-2 ratio and preventing proteolytic activities. *Mol. Cancer*, **3**, 36.

Degen, J.W., Walbridge, S., Vortmeyer, A.O., Oldfield, E.H. & Lonser, R.R. (2003) Safety and efficacy of convection-enhanced delivery of gemcitabine or carboplatin in a malignant glioma model in rats. *J. Neurosurg.*, **99**, 893-898.

Delva, L., Cornic, M., Balitrand, N., Guidez, F., Miclea, J.M., Delmer, A., Teillet, F., Fenaux, P., Castaigne, S., Degos, L. & Chomienne, C. (1993) Resistance to all-trans retinoic acid (ATRA) therapy in relapsing acute promyelocytic leukemia: study of in vitro ATRA sensitivity and cellular retinoic acid binding protein levels in leukemic cells. *Blood*, **82**, 2175-2181.

Flynn, P.J., Miller, W.J., Weisdorf, D.J., Arthur, D.C., Brunning, R. & Branda, R.F. (1983) Retinoic acid treatment of acute promyelocytic leukemia: in vitro and in vivo observations. *Blood*, **62**, 1211-1217.

Greish, K. (2007) Enhanced permeability and retention of macromolecular drugs in solid tumors: a royal gate for targeted anticancer nanomedicines. *J. Drug Target*, **15**, 457-464.

Hamaguchi, T., Kato, K., Yasui, H., Morizane, C., Ikeda, M., Ueno, H., Muro, K., Yamada, Y., Okusaka, T., Shirao, K., Shimada, Y., Nakahama, H. & Matsumura, Y. (2007) A phase I and pharmacokinetic study of NK105, a paclitaxel-incorporating micellar nanoparticle formulation. *Br. J. Cancer*, **97**, 170-176.

Inoue, T., Yamashita, Y., Nishihara, M., Sugiyama, S., Sonoda, Y., Kumabe, T., Yokoyama, M. & Tominaga, T. (2009) Therapeutic efficacy of a polymeric micellar doxorubicin infused by convection-enhanced delivery against intracranial 9L brain tumor models. *Neuro. Oncol.*, **11**, 151-157.

Jaeckle, K.A., Hess, K.R., Yung, W.K., Greenberg, H., Fine, H., Schiff, D., Pollack, I.F., Kuhn, J., Fink, K., Mehta, M., Cloughesy, T., Nicholas, M.K., Chang, S. & Prados, M. (2003) Phase II evaluation of temozolomide and 13-cis-retinoic acid for the treatment of recurrent and progressive malignant glioma: a North American Brain Tumor Consortium study. *J. Clin. Oncol.*, **21**, 2305-2311.

Kikuchi, T., Saito, R., Sugiyama, S., Yamashita, Y., Kumabe, T., Krauze, M., Bankiewicz, K. & Tominaga, T. (2008) Convection-enhanced delivery of polyethylene glycol-coated liposomal doxorubicin: characterization and efficacy in rat intracranial glioma models. *J. Neurosurg.*, **109**, 867-873.

Koizumi, F., Kitagawa, M., Negishi, T., Onda, T., Matsumoto, S., Hamaguchi, T. & Matsumura, Y. (2006) Novel SN-38-incorporating polymeric micelles, NK012, eradicate vascular endothelial growth factor-secreting bulky tumors. *Cancer Res.*, **66**, 10048-10056.

Kunwar, S., Prados, M.D., Chang, S.M., Berger, M.S., Lang, F.F., Piepmeier, J.M., Sampson, J.H., Ram, Z., Gutin, P.H., Gibbons, R.D., Aldape, K.D., Croteau, D.J., Sherman, J.W. & Puri, R.K. (2007) Direct intracerebral delivery of cintredekin besudotox (IL13-PE38QQR) in recurrent malignant glioma: a report by the Cintredekin Besudotox Intraparenchymal Study Group. *J. Clin. Oncol.*, **25**, 837-844.

Kuroda, J., Kuratsu, J., Yasunaga, M., Koga, Y., Saito, Y. & Matsumura, Y. (2009) Potent anticancer effect of SN-38-incorpotrating polymeric micelle, NK012, against malignant glioma. *Int. J. Cancer*, **124**, 2505-2511.

MacKay, J.A., Deen, D.F. & Szoka, F.C., Jr. (2005) Distribution in brain of liposomes after convection enhanced delivery; modulation by particle charge, particle diameter, and presence of steric coating. *Brain Res.*, **1035**, 139-153.

Noble, C.O., Krauze, M.T., Drummond, D.C., Yamashita, Y., Saito, R., Berger, M.S., Kirpotin, D.B., Bankiewicz, K.S. & Park, J.W. (2006) Novel nanoliposomal CPT-11 infused by convection-enhanced delivery in intracranial tumors: pharmacology and efficacy. *Cancer Res.*, **66**, 2801-2806.

Saito, R., Bringas, J.R., McKnight, T.R., Wendland, M.F., Mamot, C., Drummond, D.C., Kirpotin, D.B., Park, J.W., Berger, M.S. & Bankiewicz, K.S. (2004) Distribution of liposomes into brain and rat brain tumor models by convection-enhanced delivery monitored with magnetic resonance imaging. *Cancer Res.*, **64**, 2572-2579.

Saito, R., Krauze, M.T., Noble, C.O., Drummond, D.C., Kirpotin, D.B., Berger, M.S., Park, J.W. & Bankiewicz, K.S. (2006a) Convection-enhanced delivery of Ls-TPT enables an effective, continuous, low-dose chemotherapy against malignant glioma xenograft model. *Neuro. Oncol.*, **8**, 205-214.

Saito, R., Krauze, M.T., Noble, C.O., Tamas, M., Drummond, D.C., Kirpotin, D.B., Berger, M.S., Park, J.W. & Bankiewicz, K.S.

(2006b) Tissue affinity of the infusate affects the distribution volume during convection-enhanced delivery into rodent brains: implications for local drug delivery. *J. Neurosci. Methods*, **154**, 225-232.

Satoh, T., Higuchi, Y., Kawakami, S., Hashida, M., Kagechika, H., Shudo, K. & Yokoyama, M. (2009) Encapsulation of the synthetic retinoids Am80 and LE540 into polymeric micelles and the retinoids' release control. *J. Control Release*, **136**, 187-195.

Schneider, S.M., Offterdinger, M., Huber, H. & Grunt, T.W. (2000) Activation of retinoic acid receptor a is sufficient for ful induction of retinoid responses in SK-BR-3 and T47D Human brest cancer cells. *Cancer Res.*, **60**, 5479-5487.

Shapiro, W.R. & Young, D.F. (1984) Neurological complications of antineoplastic therapy. *Acta Neurol. Scand. Suppl.*, **100**, 125-132.

Sonoda, Y., Ozawa, T., Aldape, K.D., Deen, D.F., Berger, M.S. & Pieper, R.O. (2001) Akt pathway activation converts anaplastic astrocytoma to glioblastoma multiforme in a human astrocyte model of glioma. *Cancer Res.*, **61**, 6674-6678.

Tobita, T., Takeshita, A., Kitamura, K., Ohnishi, K., Yanagi, M., Hiraoka, A., Karasuno, T., Takeuchi, M., Miyawaki, S., Ueda, R., Naoe, T. & Ohno, R. (1997) Treatment with a new synthetic retinoid, Am80, of acute promyelocytic leukemia relapsed from complete remission induced by all-trans retinoic acid. *Blood*, **90**, 967-973.

Tsukioka, Y., Matsumura, Y., Hamaguchi, T., Koike, H., Moriyasu, F. & Kakizoe, T. (2002) Pharmaceutical and biomedical differences between micellar doxorubicin (NK911) and liposomal doxorubicin (Doxil). *Jpn. J. Cancer Res.*, **93**, 1145-1153.

Uchino, H., Matsumura, Y., Negishi, T., Koizumi, F., Hayashi, T., Honda, T., Nishiyama, N., Kataoka, K., Naito, S. & Kakizoe, T. (2005) Cisplatin-incorporating polymeric micelles (NC-6004) can reduce nephrotoxicity and neurotoxicity of cisplatin in rats. *Br. J. Cancer*, **93**, 678-687.

Vogelbaum, M.A. (2007) Convection enhanced delivery for treating brain tumors and selected neurological disorders: symposium review. *J. Neurooncol.*, **83**, 97-109.

Wismeth, C., Hau, P., Fabel, K., Baumgart, U., Hirschmann, B., Koch, H., Jauch, T., Grauer, O., Drechsel, L., Brawanski, A., Bogdahn, U. & Steinbrecher, A. (2004) Maintenance therapy with 13-cis retinoid acid in high-grade glioma at complete response after first-line multimodal therapy—a phase-II study. *J. Neurooncol.*, **68**, 79-86.

Yamashita, Y., Krauze, M.T., Kawaguchi, T., Noble, C.O., Drummond, D.C., Park, J.W. & Bankiewicz, K.S. (2007) Convection-enhanced delivery of a topoisomerase I inhibitor (nanoliposomal topotecan) and a topoisomerase II inhibitor (pegylated liposomal doxorubicin) in intracranial brain tumor xenografts. *Neuro. Oncol.*, **9**, 20-28.

Yokoyama, M., Miyauchi, M., Yamada, N., Okano, T., Sakurai, Y., Kataoka, K. & Inoue, S. (1990) Characterization and anticancer activity of the micelle-forming polymeric anticancer drug adriamycin-conjugated poly(ethylene glycol)-poly(aspartic acid) block copolymer. *Cancer Res.*, **50**, 1693-1700.

Yokoyama, M., Okano, T., Sakurai, Y., Fukushima, S., Okamoto, K. & Kataoka, K. (1999) Selective delivery of adriamycin to a solid tumor using a polymeric micelle carrier system. *J. Drug Target.*, **7**, 171-186.

Yung, W.K., Kyritsis, A.P., Gleason, M.J. & Levin, V.A. (1996) Treatment of recurrent malignant gliomas with high-dose 13-cis-retinoic acid. *Clin. Cancer Res.*, **2**, 1931-1935.

Gamma Knife radiosurgery for hemangiomas of the cavernous sinus: a seven-institute study in Japan

Clinical article

Masaaki Yamamoto, M.D.,[1] Yoshihisa Kida, M.D.,[2] Seiji Fukuoka, M.D.,[3] Yoshiyasu Iwai, M.D.,[4] Hidefumi Jokura, M.D.,[5] Atsuya Akabane, M.D.,[6] and Toru Serizawa, M.D.[7]

Departments of Neurosurgery, [1]Katsuta Hospital Mito GammaHouse, Hitachi-naka; [2]Komaki City Hospital, Komaki; [3]Nakamura Memorial Hospital, Sapporo; [4]Osaka City General Hospital, Osaka; [5]Furukawa Seiryo Hospital, Oskai; [6]Kanto Medical Center NTT EC, Tokyo; and [7]Chiba Cardiovascular Center, Ichihara, Japan

Object. Gamma Knife radiosurgery (GKS) is currently used for primary or postoperative management of cavernous sinus (CS) hemangiomas. The authors describe their experience with 30 cases of CS hemangioma successfully managed with GKS.

Methods. Thirty patients with CS hemangiomas, including 19 female and 11 male patients with a mean age of 53 years (range 19–78 years) underwent GKS at 7 facilities in Japan. Pathological entity was confirmed using surgical specimens in 17 patients, and neuroimaging diagnosis only in 13. Eight patients were asymptomatic before GKS, while 22 had ocular movement disturbances and/or optic nerve impairments. The mean tumor volume was 11.5 cm^3 (range 1.5–51.4 cm^3). The mean dose to the tumor periphery was 13.8 Gy (range 10.0–17.0 Gy).

Results. The mean follow-up period was 53 months (range 12–138 months). Among the 22 patients with symptoms prior to GKS, complete remission was achieved in 2, improvement in 13, and no change in 7. Hemifacial sensory disturbance developed following GKS in 1 patient. The most recent MR images showed remarkable shrinkage in 18, shrinkage in 11, and no change in 1 patient.

Conclusions. Gamma Knife radiosurgery proved to be an effective treatment strategy for managing CS hemangiomas. Given the diagnostic accuracy of recently developed neuroimaging techniques and the potentially serious bleeding associated with biopsy sampling or attempted surgical removal, the authors recommend that GKS be the primary treatment in most patients who have a clear neuroimaging diagnosis of this condition.
(DOI: 10.3171/2009.6.JNS08271)

Key Words • **cavernous sinus** • **hemangioma** • **radiosurgery** • **Gamma Knife**

Despite past confusion regarding the clinical entity of CS hemangiomas,[1] Gonzalez et al.[3] recently reported that this condition is now recognized as a histologically benign vascular tumor with characteristics completely different from those of intracerebral carvernous angiomas, which are vascular malformations. Recent advancements in neuroimaging techniques have allowed precise diagnosis of hemangiomas involving the CS prior to treatment.[7,16,20] The ideal treatment for CS hemangiomas, whether symptomatic or incidental, has long been total microsurgical resection.[8] However, because they involve extremely complex anatomical structures and tend to bleed excessively when removed, or even with attempted biopsy sampling, reported surgical results are still unfavorable,[9,14,21] i.e., relatively low rates of total removal, though with negligible morbidity rates, even when recently recommended surgical techniques are applied; the extradural approach[2,17] and induced systemic hypotension.[11] For cases in which total removal cannot be achieved, fractionated radiotherapy for the residual tumors has been recommended.[15] At present, GKS is being used for primary or postoperative management of patients with CS hemangiomas and favorable treatment results have been reported.[5,6,10,12,13,18] However, the incidence of this condition is extremely low. Thus, the small number of reported cases prompted this multiinstitutional analysis of the authors' experiences. Fortunately, GKS is relatively uniform such that treatment techniques using basically the same equipment vary little among institutes. Thus, GKS is considered to be suitable for a multiinstitutional study.

The authors describe 30 patients with CS hemangiomas who were successfully managed with GKS in our 7 institutes in Japan. All 7 facilities started performing

Abbreviations used in this paper: CS = cavernous sinus; GKS = Gamma Knife radiosurgery.

TABLE 1: Summary of characteristics in 30 patients*

Case No.	Age at GKS (yrs), Sex	Initial Presentation	Surgery Pre-GKS	CN Symptoms Pre-GKS	Tumor Vol (cm^3)	Min Dose (Gy)	Length of FU (mos)	Symptom Changes Post-GKS	Most Recent MR Findings
1	33, M	diplopia	no	III	5.2	15.00	30	resolved	remarkable shrinkage
2	54, F	incidental	no	none	3.5	16.00	30	none	remarkable shrinkage
3	44, M	incidental	yes	III	12.3	13.00	50	resolved	shrinkage
4	54, F	incidental	no	none	4.1	13.00	30	none	shrinkage
5	48, M	diplopia	yes	III, IV, V	8.5	13.00	27	improved	no change
6	50, F	ocular pain	no	III, V	1.5	16.20	138	improved	remarkable shrinkage
7	38, F	diplopia	yes	II, VI	3.4	17.00	116	stable	remarkable shrinkage
8	66, F	incidental	yes	II, III, IV, VI	11.1	14.00	83	stable	shrinkage
9	73, F	diplopia	no	II, III	7.7	16.00	78	improved	shrinkage
10	69, F	decreased visual acuity	yes	II, III, IV, V, VI	39.7	10.00	56	stable	shrinkage
11	77, M	ocular pain	yes	III	11.9	13.00	43	stable	shrinkage
12	67, F	diplopia	no	none	19.7	12.50	41	none	shrinkage
13	59, M	decreased visual acuity	yes	II, III	33.4	11.0 × 2†	26	improved	shrinkage
14	46, M	diplopia	yes+RT	none	51.4	15.00‡	84	none	remarkable shrinkage
15	68, F	diplopia	yes	III	6.0	12.00	74	stable	shrinkage
16	54, F	headache	no	none	10.5	15.00	64	none	shrinkage
17	54, F	incidental	yes	none	10.2	15.00	24	none	remarkable shrinkage
18	78, F	diplopia	yes	III	8.5	15.00	52	improved	remarkable shrinkage
19	51, F	diplopia	no	VI	7.9	14.00	26	improved	remarkable shrinkage
20	61, M	diplopia	yes	VI	2.9	16.00	81	improved	remarkable shrinkage
21	45, F	diplopia	no	VI	3.9	15.00	25	improved	remarkable shrinkage
22	46, M	diplopia	no	III	4.9	15.00	13	improved	remarkable shrinkage
23	50, F	diplopia	no	III, IV, VI	19.0	10.00	38	improved	remarkable shrinkage
24	54, F	diplopia	no	III	6.4	16.00	57	improved	remarkable shrinkage
25	35, F	decreased visual acuity	no	II	4.5	12.00	12	improved	remarkable shrinkage
26	19, M	diplopia	yes	none	1.9	14.00	36	none	remarkable shrinkage
27	40, M	diplopia, facial numbness	yes	III, V, VI	5.3	12.00	96	stable	remarkable shrinkage
28	58, F	headache	yes	II	13.6	10.00	52	improved	remarkable shrinkage
29	51, F	diplopia	yes	III	20.8	8.0 × 2†	66	stable	shrinkage
30	56, M	diplopia	yes	none	4.9	12.00	48	none	remarkable shrinkage

* CN = cranial nerve; FU = follow-up; RT = radiation therapy.
† Indicates 2-stage GKS.
‡ Indicates partial coverage.

GKS between 1991 and 1998. Each of the study authors, all of whom are chief neurosurgeons at their facilities, has more than 10 years of GKS experience and each has treated more than 3000 patients with a GK.

Methods

Thirty patients who underwent GKS at 7 GK facilities in Japan and who were followed using MR imaging for 12 months or more after treatment were studied (Table 1). All patients signed consent forms allowing their data to be used, after the study had been fully explained. Five (Cases 6, 7, 8, 18, and 27) of these 30 patients have been described elsewhere[5,6,10,13] but are included in this study with further long-term follow-up results. As summarized in Table 1, there were 19 female and 11 male patients with a mean age at the time of GKS of 53 years (range 19–78 years). The most common initial presentation was ocular

TABLE 2: Summary of postsurgical changes in symptoms (17 patients)

Preop Symptoms	Ocular Movement Disturbance	Decreased Visual Acuity	Ocular Pain/ Headaches	No Deficits	Total (%)
no. of patients	10	2	2	3	17
improved	3	0	0	0	3 (17.6)
no changes	3	0	0	1	4 (23.5)
additional disturbance	4	2	2	2	10 (58.8)

TABLE 3: Summary of postradiosurgical changes in symptoms (30 patients)

Symptoms Pre-GKS	Ocular Movement Disturbance	Decreased Visual Acuity	Both*	No Deficits	Total (%)
no. of patients	15	2	5	8	30
recovery	2*	0	0	0	2† (6.7)
improved	9	2	2	0	13 (43.3)
no changes	4	0	3	8	15 (50.0)
additional disturbance	1†	0	0	0	1† (3.3)

* Indicates both ocular movement disturbance and decreased visual acuity.

† Ocular movement recovered completely but additional trigeminal nerve disturbance occurred in 1 patient.

movement disturbances, seen in 18 patients (60.0%). One of the 18 patients had hemifacial sensory disturbance, 4 (13.3%) ocular pain and/or headache, and 3 (10.0%) visual disturbances. The remaining 5 patients were asymptomatic.

Prior to GKS, surgical removal was performed in 17 patients, one of whom underwent postoperative fractionated radiotherapy (Case 14). The nature of the pathological entity was confirmed using surgical specimens in these 17 patients and neuroimaging diagnosis only in 13. Postoperative symptom changes are shown in Table 2. Among 10 patients with ocular movement disturbances, symptom palliation was achieved in 3, there were no changes in 3, and additional neurological deficits developed in the remaining 4. Additional ocular movement disturbances occurred postoperatively in 2 patients with preoperative visual disturbances. Among the remaining 5 patients with no neurological deficits, additional ocular movement disturbances developed postoperatively in 3, and visual disturbance in 1. These postoperative results can be summarized as follows: no neurological deficits before or after surgery in 1 patient (5.9%), improvement in 3 (17.6%), no change in 3 (17.6%), and worsening in 10 patients (58.8%).

Eight patients were asymptomatic before GKS, while 15 had ocular movement disturbances, 2 had optic nerve impairments, and 5 patients had both. The mean tumor volume was 11.5 cm^3 (range 1.5–51.4 cm^3). Due to the relatively large tumor volumes, staged GKS with intervals of a few weeks was applied in 2 patients (the selected dose at the tumor periphery was 11.0 Gy each time for the patient in Case 13, and 8.0 Gy for the patient in Case 29), and only the tumor base was irradiated in 1 patient (Case 14). In all other patients, the entire tumor volume was fully covered with a 50–60% isodose gradient, and the mean and median doses at the tumor periphery were 13.8 Gy and 14.0 Gy, respectively (range 10.0–17.0 Gy).

Results

All 30 patients underwent periodic MR imaging follow-up. The mean and median follow-up periods after GKS were 53 and 49 months, respectively (range 12–138 months). The most recent MR images demonstrated remarkable tumor shrinkage (> 50% tumor volume reduction) in 18 patients (60.0%), slight shrinkage in 11 (36.7%) and no change in 1 (3.3%). No tumors showed transient enlargement after GKS. In the 18 tumors in which remarkable shrinkage was attained, a marked tumor volume decrease had occurred by 12 months after GKS. To date, no patients have experienced tumor recurrence.

Post-GKS changes in neurological symptoms are listed in Table 1 and summarized in Table 3. Among the 20 patients with ocular movement disturbances, including 5 who also had visual disturbances, complete remission of symptoms was obtained in 2, improvement in 12, and no change in 6. Additional trigeminal nerve disturbance occurred in 1 patient (Case 3). Among the 7 patients with visual disturbances (including the 5 with ocular movement disturbances), improvement was noted in 4 and no change in 3. Thus, among the 22 patients with cranial neuropathy before GKS, complete remission was achieved in 2 (9.1%), improvement in 13 (59.1%), and no change in 7 (31.8%). No additional disturbances occurred in the remaining 8 patients who did not have neurological deficits before GKS.

Illustrative Cases

Case 14

Presentation and First Operation. In 1982, an ophthalmologist recommended further examination after this 29-year-old man presented with diplopia. At another institution, neurological examination revealed left oculomotor nerve paresis and a left CS tumor was demonstrated on CT. The patient received a preoperative diagnosis of meningioma and underwent craniotomy, despite failed biopsy sampling due to massive bleeding. The patient's symptoms subsided after steroid treatment.

Second Operation. In 1995, left oculomotor nerve paresis recurred and MR images obtained on January 17, 1996, demonstrated the presence of a left CS tumor extending into the middle fossa (Fig. 1A). The patient underwent a left frontotemporal craniotomy followed by biopsy sampling. Because of massive hemorrhaging, however,

TABLE 4: Summary of the 16 cases reported in the literature*

Authors & Yr	Age at GKS (yrs), Sex	CN Symptoms Pre-GKS	Tumor Vol (cm^3)	Min Dose (Gy)	Length of FU (mos)	Symptom Changes Post-GKS	Tumor Vol at Latest FU (cm^3)	Vol Reduction Rate (%)
Iwai et al., 1999	40, M	III, V, VI	5.3	12.0	20	no change	shrinkage	NA
Thompson et al., 2000	24, F	III	5.6	14.0	24	improved	0.8	14
	14, F	V, VI, VII	5.2	19.0	18	improved	0.9	17
	44, M	III, IV	10.8	15.0	12	improved	10.9	101
Seo et al., 2000	79, F	III, IV	8.5	15.0	24	recovery	shrinkage	NA
Kida et al., 2001	50, F	III, V	1.5	16.2	33	no change	0.7	47
	38, F	II, VI	3.4	17.0	36	improved	1.4	41
	66, F	II, III, IV, VI	11.1	14.0	12	no change	5.1	46
Nakamura et al., 2002	75, F	II, III	9.5	12.0–14.0†	60	improved	4.3	45
	68, F	II	3.3	12.0–14.0†	48	no change	3.0	91
	55, F	none	6.6	12.0–14.0†	24	none	4.6	70
Peker et al., 2004	39, F	none	3.8	15.0	52	none	1.5	39
	60, M	III	5.8	16.0	32	no change	2.1	36
	37, M	V, VI	6.2	15.0	45	improved	1.3	21
	39, F	III, V	4.6	15.0	29	improved	1.1	24
	44, M	II, III	4.4	14.0	6	no change	1.7	39

* NA = not applicable.

† The selected dose for the individual patient was not described.

an attempt at tumor removal had to be discontinued. The pathological report was consistent with a hemangioma. Postoperatively, the patient received fractionated radiotherapy with a total dose of 51 Gy, and significant tumor shrinkage was noted on follow-up MR imaging (Fig. 1B). His oculomotor function gradually improved after radiotherapy, eventually normalizing.

Gamma Knife Radiosurgery. Although there was no neurological deterioration, MR images obtained 60 months posttreatment demonstrated apparent regrowth of the tumor (Fig. 1C). The patient underwent GKS at the Katsuta Hospital Mito GammaHouse on January 19, 2000. Because of prior radiotherapy and a relatively large tumor volume (51.4 cm^3) the lower half of the tumor was covered with a 50% isodose gradient and irradiation was administered with the maximum dose of 30.0 Gy; that is, 56% of the entire tumor received a radiation dose of ≥ 15.0 Gy. The patient's neurological status has been stable since radiosurgery. Follow-up MR images obtained 6 months after GKS revealed remarkable shrinkage through the 12th postradiosurgical month and confirmed the absence of growth thereafter up to the most recent follow-up MR imaging studies obtained 84 months after radiosurgery (Figs. 1D and E and 2).

Case 15

This 68-year-old woman presented with a 3-month history of diplopia, and further examination was recommended by the ophthalmologist. At another institution (not one of the 7 GKS institutions), neurological examination revealed right oculomotor nerve paresis and a right CS tumor was demonstrated on MR imaging. Biopsy sampling through a frontotemporal craniotomy was performed, and the lesion was confirmed to be consistent with a hemangioma.

The patient underwent GKS at the Katsuta Hospital Mito GammaHouse on August 7, 2001. The tumor, with a volume of 6.0 cm^3, was covered with a 60% isodose gradient and irradiated with a peripheral dose of 12.0 Gy (Fig. 3A). Postradiosurgically, to date, her oculomotor nerve function has remained unchanged. Follow-up MR images obtained 6 months after GKS showed a slight shrinkage of the lesion that continued through the 12th postradiosurgical month, and absence of growth was confirmed thereafter up to the most recent follow-up MR imaging, conducted 74 months after GKS (Fig. 3B and C).

Case 16

This 54-year-old woman presented to an outside institution with a 2-month history of headaches. Neuroimaging examinations showed typical findings of a hemangioma involving the left CS. Her headaches were nonspecific and not considered to be caused by the tumor. Therefore, a watch and wait approach was recommended. However, the patient was extremely concerned about not being treated, and GKS was therefore undertaken at Katsuta Hospital Mito GammaHouse on February 9, 2002. The tumor, with a volume of 10.5 cm^3, was covered with a 60% isodose gradient and irradiated with a maximum dose of 25.0 Gy (the entire tumor received an irradiation dose of 15.0 Gy or more; Fig. 4 *left*). Periodic follow-up MR images showed slight shrinkage. No growth has been seen to date, with the most recent follow-up MR images having been obtained 64 months after radiosurgery (Fig. 4 *right*).